Accepted Manuscript

Neuroprotective effects of benzyloxy substituted small molecule monoamine oxidase B inhibitors in Parkinson's disease

Zhimin Wang, Jiajia Wu, Xuelian Yang, Pei Cai, Qiaohong Liu, Kelvin D.G. Wang, Lingyi Kong, Xiaobing Wang

PII: S0968-0896(16)30768-4
DOI: http://dx.doi.org/10.1016/j.bmc.2016.09.050
Reference: BMC 13303

To appear in: *Bioorganic & Medicinal Chemistry*

Received Date: 8 August 2016
Revised Date: 19 September 2016
Accepted Date: 20 September 2016

Please cite this article as: Wang, Z., Wu, J., Yang, X., Cai, P., Liu, Q., Wang, K.D.G., Kong, L., Wang, X., Neuroprotective effects of benzyloxy substituted small molecule monoamine oxidase B inhibitors in Parkinson's disease, *Bioorganic & Medicinal Chemistry* (2016), doi: http://dx.doi.org/10.1016/j.bmc.2016.09.050

Neuroprotective effects of benzyloxy substituted small molecule monoamine oxidase B inhibitors in Parkinson's disease

Zhimin Wang [1], Jiajia Wu [1], Xuelian Yang, Pei Cai, Qiaohong Liu, Kelvin D. G. Wang, Lingyi Kong *, and Xiaobing Wang *

State Key Laboratory of Natural Medicines, Department of Natural Medicinal Chemistry, China Pharmaceutical University, 24 Tong Jia Xiang, Nanjing 210009, People's Republic of China

*Corresponding Authors: Tel/Fax: +86-25-8327-1405. E-mail: cpu_lykong@126.com; xbwang@cpu.edu.cn.

[1] These authors contributed equally.

Abstract

The benzyloxy substituted small molecules are well-known highly potent monoamine oxidase B inhibitors, but their therapeutic potential against Parkinson's disease have not been investigated in detail. In this paper, a series of representative benzyloxy substituted derivatives were synthesized and evaluated for MAO-A/B inhibition. In addition, their neuroprotective effects were investigated in 6-OHDA- and rotenone-treated PC12 cells. It was observed that most of the compounds exhibited a marked increase in survival of PC12 cells which treated with the neurotoxins. Among them, **13** exhibited remarkable and balanced neuroprotective potency. The protective effects of **13** against neurotoxins-induced apoptosis were confirmed with flow cytometry and staining methods. Furthermore, **13** also showed good BBB permeability and low toxicity according to *in vitro* BBB prediction and *in vivo* acute toxicity test. The results indicated that **13** is an effective and promising candidate to be further developed as disease-modifying drug for Parkinson's disease therapy.

Keywords:

Parkinson's disease, Monoamine oxidase, BBB permeability, Apoptosis, Neuroprotection

1. Introduction

Parkinson's disease (PD) is a degenerative disorder of the central nervous system (CNS) which characterized by a progressive loss of pigmented dopaminergic neurons in the substantia nigra pars compacta [1, 2]. The cornerstone of PD therapy is aimed at enhancing central dopamine levels with its direct metabolic precursor, L-3, 4-dihydroxyphenylalanine (L-DOPA) [3]. To enhance the therapeutic efficacy of L-DOPA and reduce the occurrence of dopamine-associated side effects, the drug is frequently administered in combination with the inhibitors that reduce the metabolism of dopamine, such as catechol-O-methyl transferase (COMT) and monoamine oxidase type B (MAO-B) inhibitors [4, 5]. Thus, inhibition of MAO-B leads to enhancement of dopaminergic neurotransmission, which considered useful in the early PD therapy [6, 7].

In the previous discovery of MAO-B inhibitors, propargylamine derivatives have been shown as selective and potent MAO-B inhibitory activities, and those compounds have been further examined neuroprotective capabilities against neurodegeneration by preventing apoptosis [8-12]. Among them, selegiline and rasagiline were successfully approved by the U. S. FDA for the treatment of PD. Both selegiline and rasagiline are used in early PD as monotherapy and adjunctive therapy to levodopa and dopamine agonists in later stages of PD. However, the clinical trials were unsuccessful to shown a clear neuroprotective action, which led to the limited usage of selegiline and rasagiline as disease-modifying drugs [13]. Therefore, the development of novel MAO-B inhibitors with potent inhibitory potency, definite therapeutic action and fewer side effects is still necessary. In fact, various benzyloxy substituted molecules as new type of excellent MAO-B inhibitors have been highly described by Petzer's group and other researchers in recent years, such as acetophenones, indoles, quinolinones, coumarins, chromones, chromanones, *a*-tetralone and phthalide analogues [14-21]. Although these benzyloxy substituted small molecules have been identified as highly potent, selective, and irreversible MAO-B inhibitors, but their therapeutic potentials against Parkinson's disease have not been investigated in detail. It is necessary to evaluate the neuroprotective activity and

molecular mechanism of these derivatives in cells model.

For this purpose, we had synthesized a series of representative benzyloxy substituted compounds with different scaffolds (**Fig 1**) and their MAO-A/B inhibitory activities had also been evaluated. In addition, these compounds were also tested for neuroprotective effects with PC12 cells model treated by 6-OHDA and rotenone, respectively. The neuroprotective effects of the preferred compounds against neurotoxins-induced apoptosis were confirmed with flow cytometry and staining method. To investigate drug-like properties, the blood-brain barrier (BBB) permeability, ADMET properties, and toxicity were also evaluated by *in vitro* and *in vivo* methods.

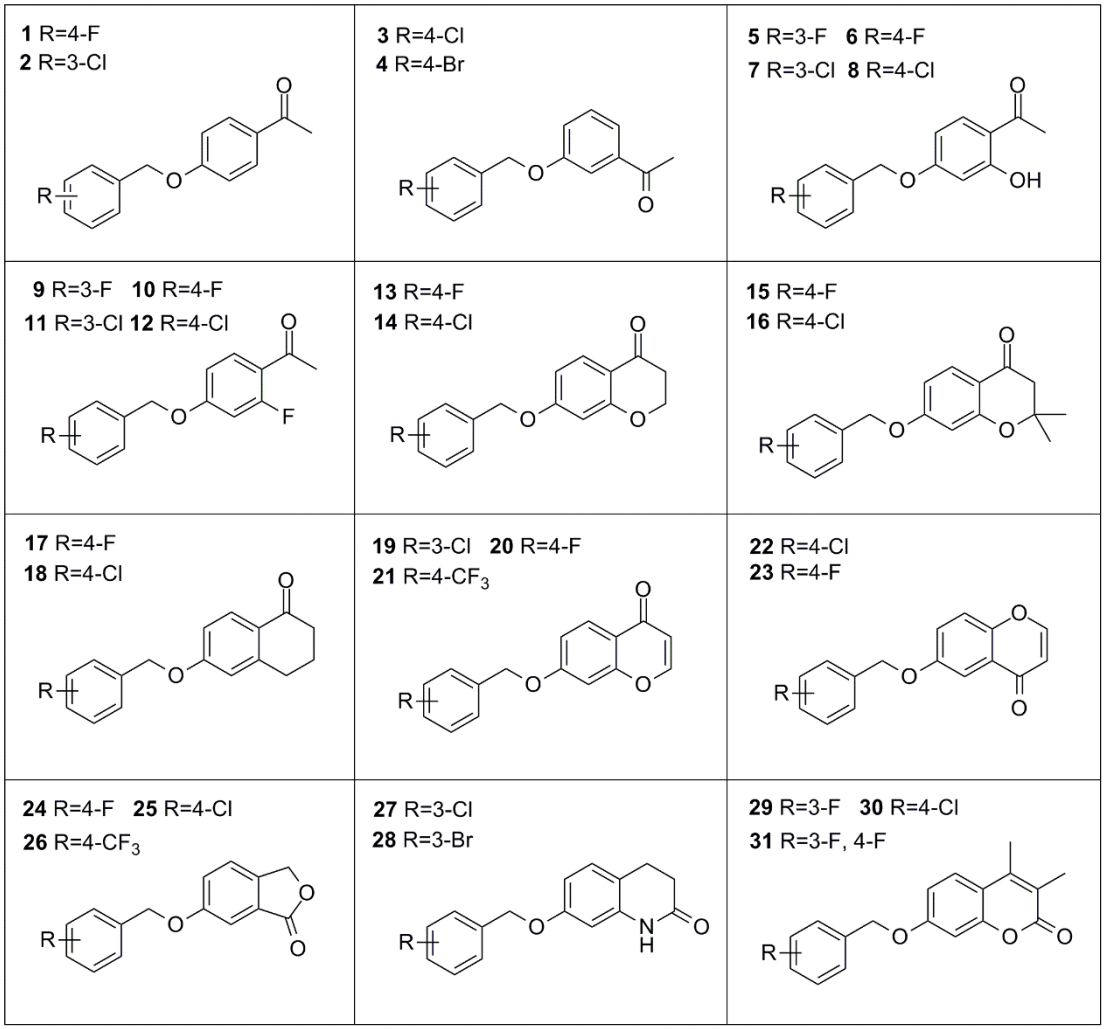

Fig 1.

2. Results and Discussion

2.1. Chemistry

These representative benzyloxy substituted derivatives (**1-31**) were efficiently synthesized along with the pathway shown in **Fig 2**. The starting materials (various skeletons, see Supporting Information for the synthesis of key intermediates **S1-4**) [17, 19, 21] reacted with the appropriate benzyl bromides in the presence of K_2CO_3 to give the target compounds in moderate to good yields.

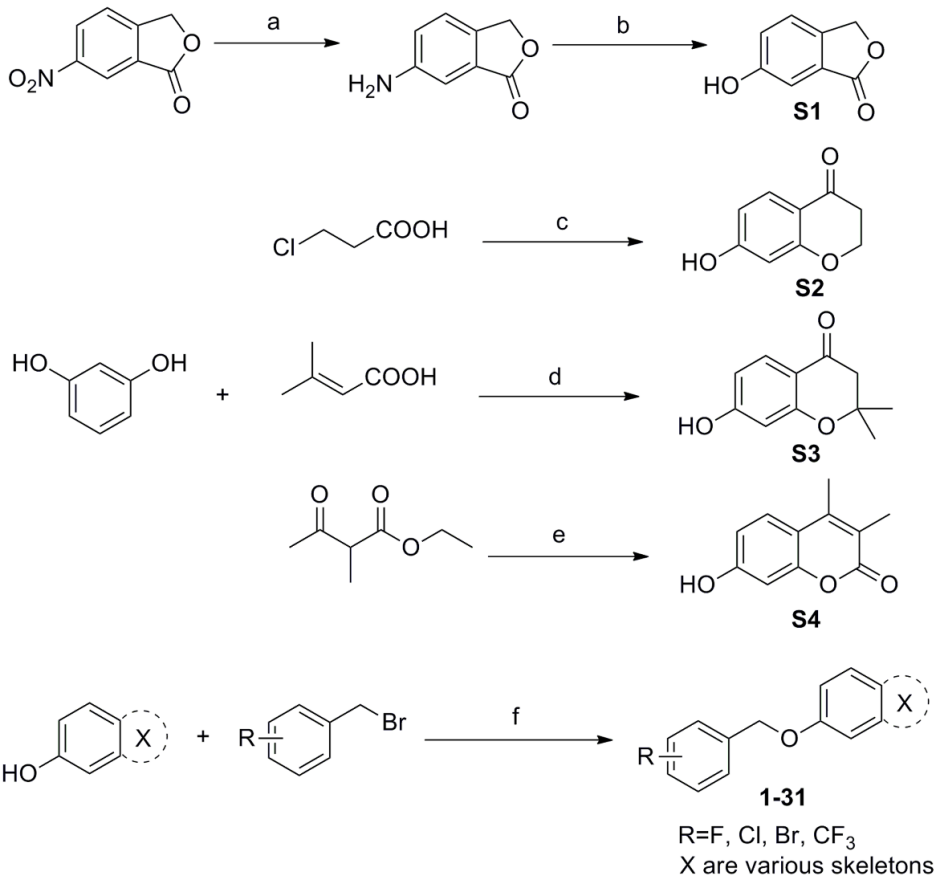

Fig 2.

2.2.Inhibition of MAOs

According to the reported assay with rasagiline and iproniazid [22-24], the MAO inhibitory activities of compounds **1-31** were explored by measuring the effects on the production of hydrogen peroxide from *p*-tyramine. As a screening result shown in **Table 1**, most of the tested compounds with C4- or C3-halogen substituted benzyloxy side chains, were selective inhibitors toward MAO-B with IC_{50} values in the

nanomolar range. The MAO-A inhibition of the tested compounds was weak with no apparent structure-activity relationship (SAR) existence. It seems that compounds bearing acetophenone and chromanone skeletons drastically decreased in MAO-A inhibition. The corresponding inhibitory activities of the reported compounds were listed in the **Table S1** (Supporting Information).

Table 1. Inhibition of human MAO-A and MAO-B activities and neuroprotective effects of compounds **1-31**.

Compounds	MAO-A	MAO-B	Selectivity	% survival of PC12 cells [c]	
	IC_{50} (μM) [a]	IC_{50} (nM) [a]	Index [b]	6-OHDA	rotenone
1	>100	15.48 ± 1.34	>6460	115.53 ± 6.57	88.59 ± 4.20
2	88.43 ± 6.90	25.32 ± 4.65	3492	123.30 ± 4.28	95.77 ± 5.08
3	39.45 ± 5.26	10.52 ± 1.04	3750	131.78 ± 3.52	109.05 ± 10.79
4	53.68 ± 2.4	92.41 ± 3.47	581	109.39 ± 3.96	105.04 ± 10.46
5	>100	41.38 ± 6.00	>2417	133.41 ± 9.23	106.30 ± 11.51
6	43.38 ± 2.15	28.42 ± 5.35	1526	143.64 ± 6.80	98.31 ± 5.73
7	48.05 ± 3.92	25.12 ± 3.50	1913	134.00 ± 10.97	93.34 ± 2.66
8	25.34 ± 7.91	42.75 ± 3.18	593	144.11 ± 10.59	105.07 ± 10.26
9	>100	96.51 ± 4.56	>1036	115.85 ± 9.35	108.75 ± 10.80
10	>100	56.89 ± 1.31	>1758	104.54 ± 8.08	113.99 ± 10.01
11	>100	13.25 ± 2.24	>7547	133.45 ± 5.85	111.85 ± 2.09
12	89.05 ± 3.9	52.93 ± 0.28	1682	141.51 ± 6.71	101.33 ± 6.58
13	>100	12.34 ± 1.62	>8104	134.19 ± 6.76	126.38 ± 6.92
14	>100	42.05 ± 2.48	>2378	143.35 ± 3.79	111.02 ± 1.89
15	>100	12.85 ± 5.38	>7782	148.17 ± 10.30	111.47 ± 4.05
16	>100	39.21 ± 2.94	>2550	143.14 ± 7.83	108.32 ± 4.12
17	1.29 ± 0.51	12.55 ± 1.68	23	139.15 ± 8.24	95.92 ± 5.40
18	0.34 ± 0.04	7.21 ± 0.81	47	126.78 ± 3.69	109.51 ± 0.71
19	23.59 ± 7.21	43.42 ± 8.25	543	117.17 ± 5.87	101.38 ± 1.73
20	18.52 ± 1.14	63.22 ± 3.54	293	124.17 ± 8.29	115.37 ± 1.82
21	18.94 ± 4.07	27.82 ± 1.35	681	122.61 ± 8.42	110.30 ± 6.00
22	4.52 ± 0.73	25.31 ± 8.21	179	122.00 ± 3.61	114.67 ± 4.26
23	13.59 ± 3.21	15.62 ± 4.29	870	114.67 ± 4.41	106.33 ± 5.61
24	1.33 ± 0.48	8.35 ± 1.01	159	116.04 ± 4.69	113.67 ± 2.27
25	3.61 ± 1.01	13.87 ± 3.14	260	137.19 ± 10.90	113.35 ± 4.58
26	9.24 ± 2.37	6.41 ± 2.73	1441	124.63 ± 6.70	111.05 ± 5.29
27	>100	14.27 ± 1.66	>7008	121.21 ± 1.52	110.21 ± 7.08
28	49.17 ± 2.73	8.17 ± 1.78	6018	111.71 ± 2.99	133.52 ± 3.24
29	>100	5.03 ± 0.81	>19881	129.93 ± 9.72	115.42 ± 7.47
30	6.77 ± 1.18	6.48 ± 1.37	1045	114.33 ± 4.81	119.33 ± 7.84
31	>100	4.25 ± 1.40	>23529	137.63 ± 3.53	116.67 ± 8.01
iproniazid	7.57 ± 0.43	8.96 ± 0.38 μM	0.84	-	-
control	-	-	-	99.33 ± 1.86	98.33 ± 3.38
rasagiline	50.71 ± 3.19	7.87 ± 1.25	6443	134.52 ± 9.09	109.03 ± 6.77

[a] IC_{50}: 50% inhibitory concentration (means ± SEM of three experiments). [b] Selectivity Index = IC_{50} (MAO-A)/IC_{50} (MAO-B). [c] Survival data are expressed as the percentage of 6-OHDA- and rotenone-treated cells. All data are the means ± SEM of at least five values measured in two independent plates.

2.3. Cytotoxicity and neuroprotection assays in PC12 cells

To investigate the safety index of these potent MAO-B inhibitors, all the compounds **1-31** were selected for cytotoxicity assay in neuroblastoma cells (PC12). After incubating the cells with the compounds for different times (24 and 72 h), the viability was investigated by the MTT [3-(4, 5-dimethyl-2-thiazolyl)-2, 5-diphenyl-2H-tetrazolium bromide] assay [25]. As shown in the **Fig 3A** and **Table S2** (Supporting Information), the results revealed that compounds **17-28** displayed low toxicities at higher concentration (100 μM), while most of the compounds at concentration of 100 and 20 μM did not shown significant neurotoxicity. This result suggested these compounds could be used for further development.

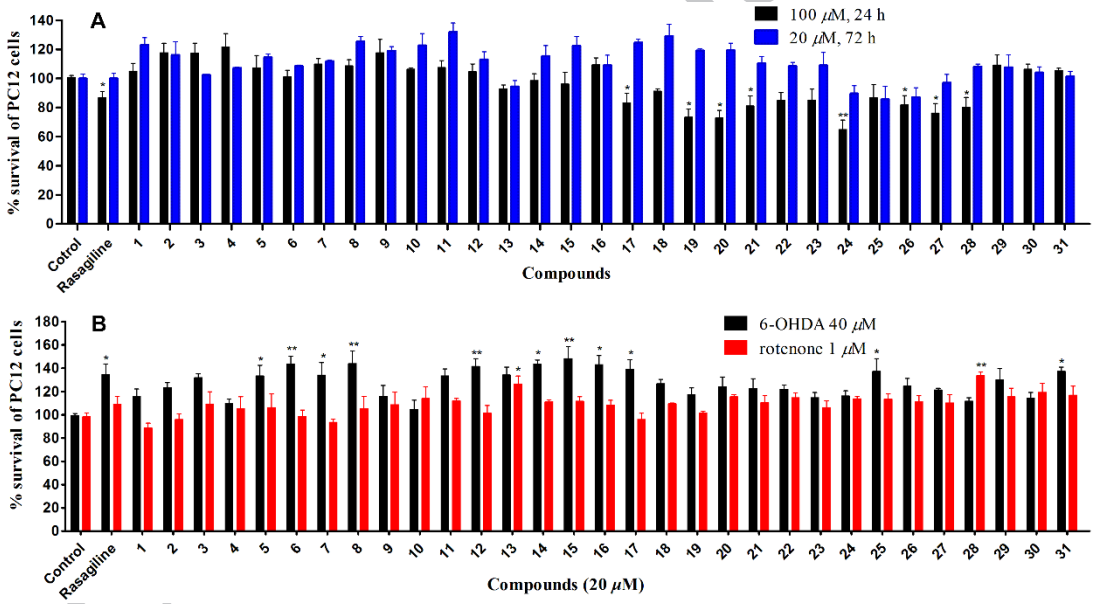

Fig 3.

To gain insight into the therapeutic potentials of these compounds, the neuroprotective capacity was also determined by MTT assay in PC12 cells. PC12 cells were chosen for this purpose due to the similarity of dopaminergic neurons, and different types of neurotoxins were used to increase the predictive value of the model for clinical neuroprotection [12]. Two parallel experiments were performed with 6-hydroxydopamine- (6-OHDA) and rotenone-treated PC12 cells [26, 27]. According to the method described by Zheng *et al.* [28] with slight modification, rasagiline was used as positive control in these experiments. Cells were incubated with 6-OHDA (40 μM)

for 24 h, and tested compounds and rasagiline were applied in a single 20 μM concentration for 1 h prior to 6-OHDA application. The MTT assay was used to assess cell viability. In the similar manner, rotenone (1 μM) was used to assess the ability of the tested compounds (20 μM) to facilitate cell survival.

As the results were summarized in **Table 1** and **Fig 3B**, rasagiline exhibited significant protective effect (39%) in 20 μM concentration in 6-OHDA-treated PC12 cell (**Table 1**) which was consistent with literature data [12, 26]. Among the tested compounds, compounds **5-8**, **12**, **14-17**, **25** and **31** were protective against 6-OHDA-induced cell death (>30% protection), while only compounds **13** and **28** shown >20% protection against rotenone-induced cell death. Especially, compound **15** showed the highest increase of 48% in the survival of 6-OHDA-treated cells. Compound **28** had the best neuroprotection (34% increased) in rotenone-induced cell death. It is worth mentioning that, compound **13**, a benzyloxy substituted chromanone hMAO-B inhibitor, was the only compound which shown effective and balanced neuroprotective activities in both 6-OHDA- and rotenone-treated PC12 cells in a concentration-dependent manner (**Fig 4**).

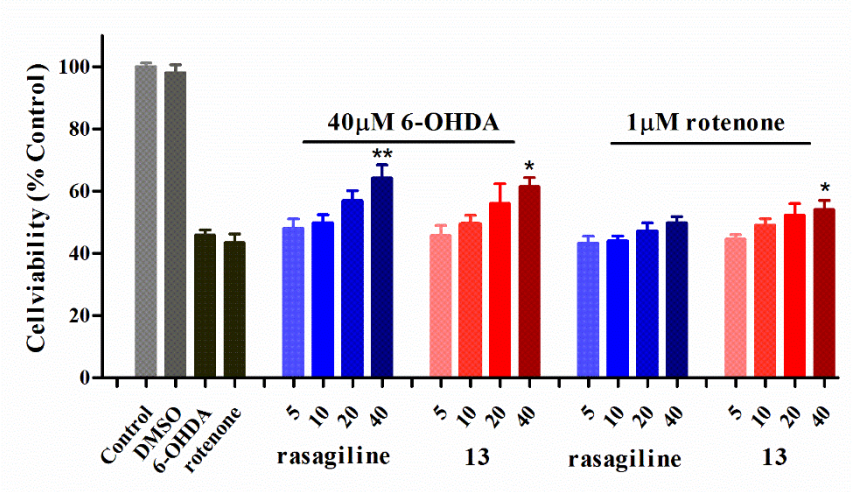

Fig 4.

2.4.Effects of compound 13 on both 6-OHDA- and rotenone-induced apoptosis in PC12 cells

Compound **13** was chosen to investigate the protective effects against neurotoxins-induced apoptosis not only because of no neurotoxicity, but also because

of its remarkable and balanced activities against both 6-OHDA- and rotenone-induced cell death. Apoptotic cells were quantified with 7-AAD and Annexin V APC dual staining method using flow cytometry [29]. The Annexin V APC (-)/7-AAD (-) population consisted primarily of normal healthy cells, while Annexin V APC (+)/7-AAD (-) cells were considered to be in the early stage of apoptosis, and Annexin V APC (+)/7-AAD (+) cells were those considered to be in the necrosis/late apoptosis stage.

Phase-contrast images **(Fig S1A** and **B**) showed that cell viability significantly decreased when cells were treated with 40 μM 6-OHDA and rotenone for 24 hours, respectively, compared with those of control. When PC12 cells were exposed to 5-40 μM compound **13** in the presence of 40 μM 6-OHDA, or 1 μM rotenone for 24 hours, the co-treated cells showed a significant increase in cell viability in a concentration dependent manner, compared to those treated with neurotoxins-treated alone. As shown in **Fig 5**, apoptotic cells percentage of 6-OHDA group were significantly increased compared to control group. In contrast, the rates of apoptotic cells were reduced when 6-OHDA-treated PC12 cells were pretreated with 5, 10, 20, 40 μM of compound **13**. As the result in **Fig 6**, PC12 cells death of rotenone-treated group was appeared due to the severe neurotoxicity. Similarly, compound **13** significantly decreased the cell death rate in a concentration dependent manner.

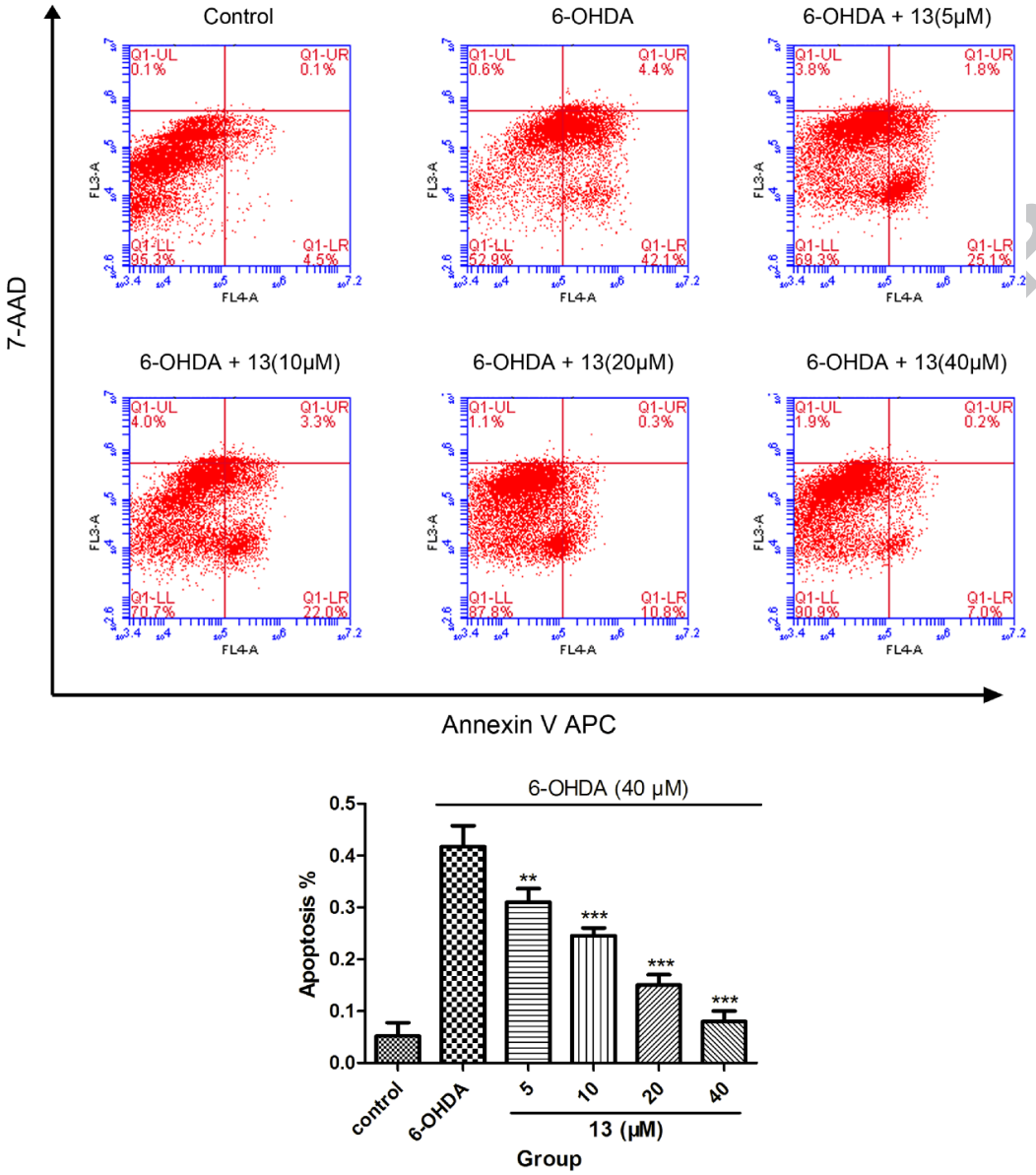
Control
6-OHDA
6-OHDA + 13(5μM)
6-OHDA + 13(10μM)
6-OHDA + 13(20μM)
6-OHDA + 13(40μM)
Q1-UL 0.1%
Q1-UR 0.1%
Q1-LL 95.3%
Q1-LR 4.5%
Q1-UL 0.6%
Q1-UR 4.4%
Q1-LL 52.9%
Q1-LR 42.1%
Q1-UL 3.8%
Q1-UR 1.8%
Q1-LL 69.3%
Q1-LR 25.1%
Q1-UL 4.0%
Q1-UR 3.3%
Q1-LL 70.7%
Q1-LR 22.0%
Q1-UL 1.1%
Q1-UR 0.3%
Q1-LL 87.8%
Q1-LR 10.8%
Q1-UL 1.9%
Q1-UR 0.2%
Q1-LL 90.9%
Q1-LR 7.0%
FL3-A
FL4-A
7-AAD
Annexin V APC
6-OHDA (40 μM)
Apoptosis %
0.0
0.1
0.2
0.3
0.4
0.5
**
***
***
***
control
6-OHDA
5
10
20
40
13 (μM)
Group

Fig 5.

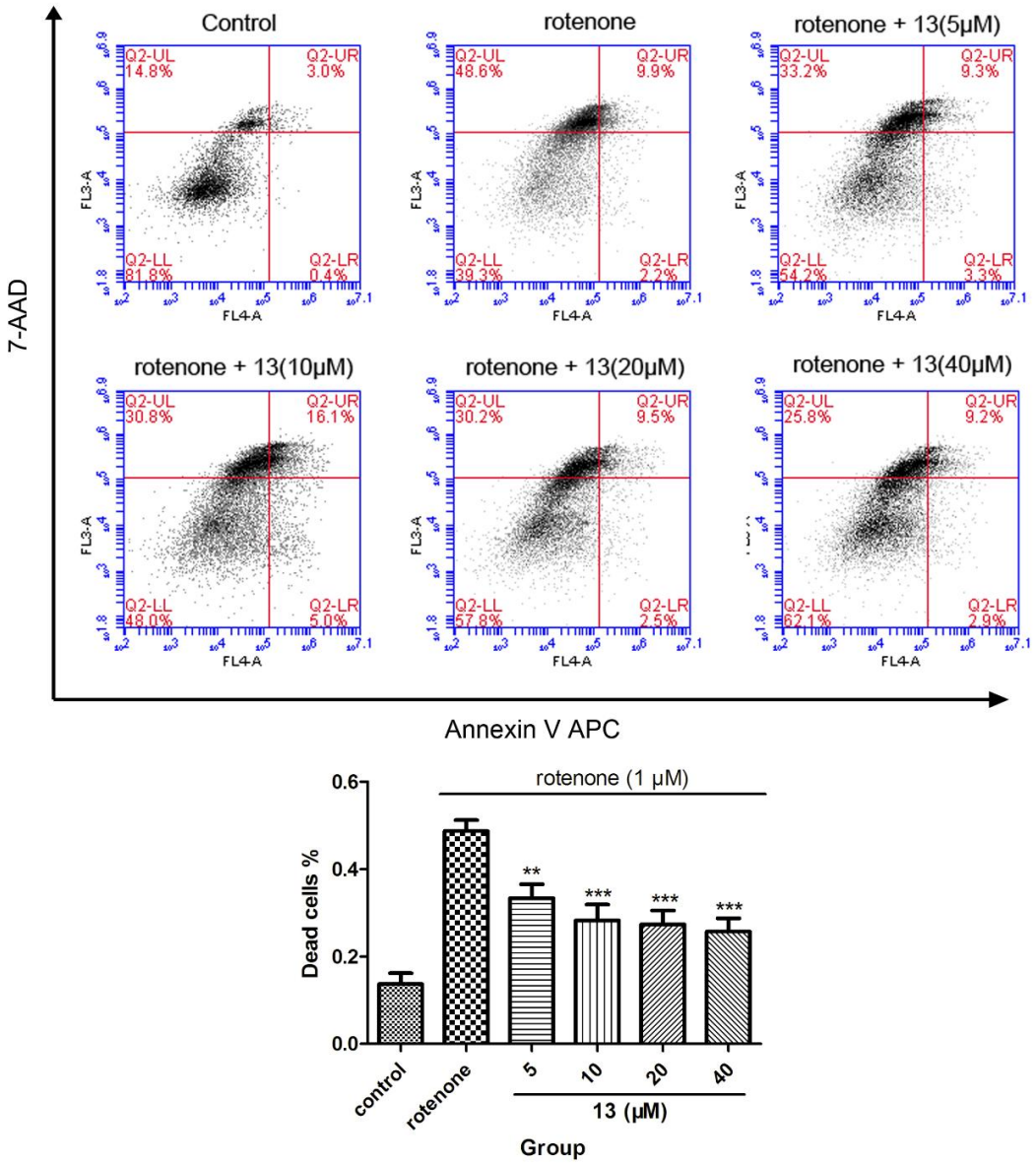

Fig 6.

Nuclear morphology characteristic of apoptosis and neuroprotection of **13** were further investigated using DNA staining with Hoechst 33258 [30]. Condensed or fragmented nuclei were characterized as apoptotic nuclei. Treatment with 20 μM compound **13** decreased the number of apoptotic nuclei (**Fig S2**). These results showed that **13** significantly decreased the percentage of apoptotic nuclei when compared to 6-OHDA- and rotenone-treated groups, which indicated that **13** have neuroprotective capability against neurodegeneration by preventing apoptosis.

2.5. Compound 13 reduced 6-OHDA- and rotenone-induced intracellular ROS accumulation

The oxidative stress caused by ROS is partly responsible for a wide variety of cellular damage and is regarded as a key initiator of neurotoxins-induced apoptotic [31]. As shown in **Fig 7**, when PC12 cells were exposed to 40 μM 6-OHDA, or 1 μM rotenone for 24 h, the intracellular ROS increased obviously by using the DCFH-DA probe. While treated with **13** at the concentrations of 5, 10 and 20 μM，the level of ROS reduced in a concentration-independent manner. This suggested that 6-OHDA and rotenone could induce ROS production and **13** effectively reduce neurotoxins-induced intracellular ROS accumulation.

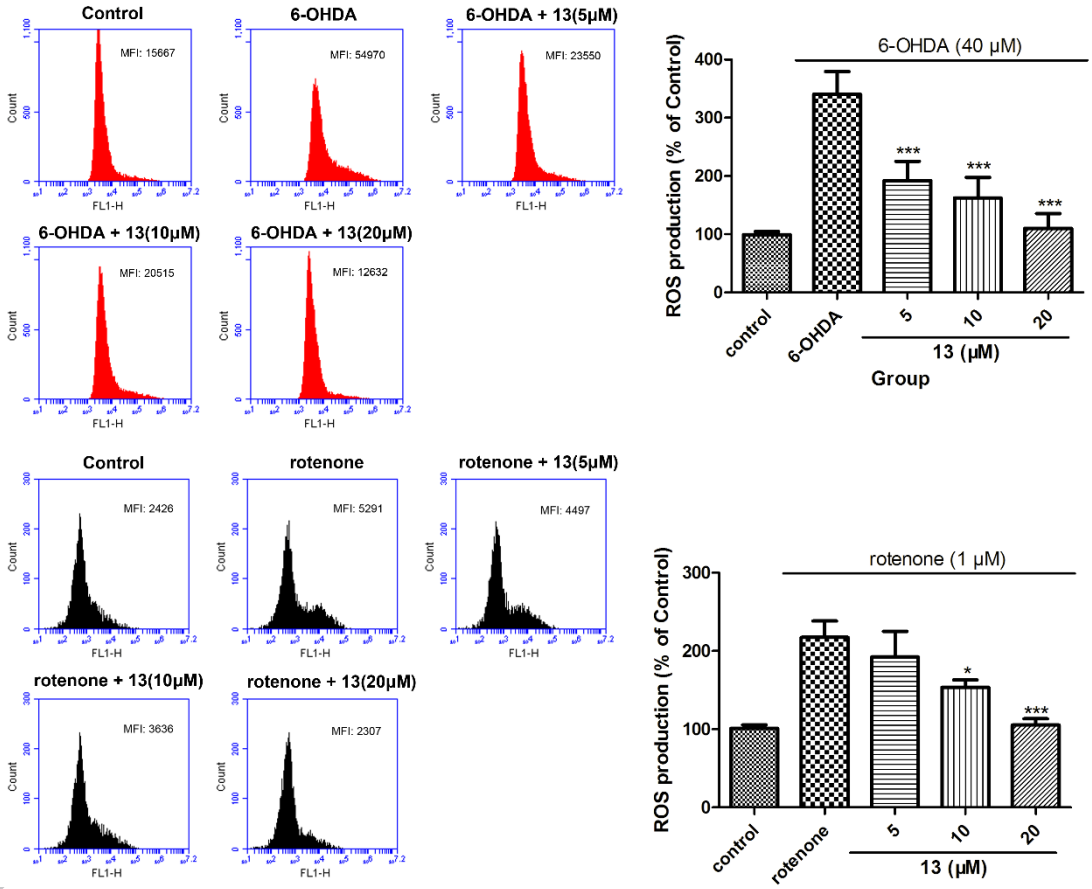

Fig 7.

2.6. Theoretical evaluation of physical properties and ADMET

The compounds with higher activity (**5-8**, **12-17**, **25** and **31**) were evaluated for the ADMET properties *in silico* by the Accelrys Discovery Studio (**Table 2**) [32]. All the compounds showed ADMET properties similar to drug rasagiline. Compared with the standard drug, these compounds were predicted to have fine absorption, high blood

brain barrier (BBB) level and good solubility. In addition, the physical properties of the selected compounds were followed Lipinski's rule of five [33]: molecular weight (MW) less than 500, the number of hydrogen bond donor atoms (HBD) less than 5, the number of hydrogen bond acceptor atoms (HBA) less than 10, the calculated logarithm of the octanol-water partition coefficient (Clog P) less than 5, and the small polar surface area less than 90 $Å^2$. However, these compounds showed a vast probability of hepatotoxicity (>0.92). The results indicated these compounds have anti-Pakinson's disease potentials which satisfied possible BBB penetration and containing drug-like properties. However, the compounds need to be further optimized for the pharmacokinetics properties.

Table 2. Physical properties and ADMET prediction of the selected compounds.

Compounds	MW [a]	Clog P [a]	HBA [a]	HBD [a]	PSA [a]	Log BB [a]	Absorption Level [b]	Solubility Level [b]	Hepatotoxicity Probability [b]	PPB Level [b]	BBB Level [b]
5	260.26	3.898	2	1	46.53	0.722496	0	3	1	0	2
6	260.26	3.898	2	1	46.53	0.722496	0	3	1	0	2
7	276.72	4.468	2	1	46.53	0.809136	0	3	1	0	2
8	276.72	4.468	2	1	46.53	0.809136	0	3	1	0	2
12	278.71	4.017	2	0	26.3	0.740584	0	2	1	0	1
13	272.28	3.656	3	0	35.53	0.685712	0	2	1	2	1
14	288.73	4.226	3	0	35.53	0.772352	0	2	1	2	1
15	300.33	4.694	3	0	35.53	0.843488	0	2	1	0	1
16	316.09	5.264	3	0	35.53	0.930128	0	2	1	1	1
17	270.30	4.256	2	0	26.3	0.776912	0	2	1	2	0
25	274.70	3.452	3	0	35.53	0.654704	0	2	1	2	1
28	332.20	4.002	2	1	38.33	0.738304	0	2	1	2	1
31	316.30	4.677	3	0	35.53	0.840904	0	2	1	1	0
rasagiline	171.24	2.344	0	1	12.03	0.664332	0	3	0	2	1
Rules	≤450	≤5.0	≤10	≤5	≤90	≥-1.0	-	-	-	-	-

[a] MW: molecular weight; C log P: calculated logarithm of the octanol-water partition coefficient; HBA: hydrogen-bond acceptor atoms; HBD: hydrogen-bond donor atoms; PSA: polar surface area; log BB = 0.0148 × PSA + 0.152 × Clog P + 0.13. [b] Absorption level (0 = good and 3 = very poor); Solubility level (0 = extremely low and 3 = good); Hepatotoxicity (0 = nontoxic and 1 = toxic); PPB, Plasma protein binding (0 = PPB < 90% and 2 = PPB > 95%); BBB level (0 = very high and 3 = low).

2.7. *In vitro* BBB permeation assay

To determine whether the promising compounds could cross BBB besides the calculated results of log BB and *in silicon* prediction, we also used a parallel artificial membrane permeation assay for BBB (PAMPA-BBB), which was described by Di *et al*. [34, 35] Assay validation was performed by comparing experimental permeability of 9 commercial drugs with reported values (**Table S4**). A plot of experimental data versus bibliographic values gave a good linear correlation: *Pe* (exp.) = 1.0976 *Pe* (bibl.) - 0.346 (R^2= 0.9537) (**Fig S3**). From the equation and taking into account the limits established by Di *et al*. for BBB permeation. The *Pe* values of these selected compounds are summarized in **Table 3**. It can be indicated that compounds **5**, **6**, **8**, **13**, **15**, **17** and **28** shown higher *Pe* values than 4.04 were able to cross the BBB.

Table 3. Permeability results (*Pe* × 10^{-6} cm s^{-1}) from the PAMPA-BBB assay for selected compounds with their predicted penetration into the CNS.

Compounds	Permeability (*Pe* × 10^{-6} cm s^{-1}) [a]	Prediction [b]
5	15.9 ± 0.6	CNS+
6	13.5 ± 0.4	CNS+
8	12.7 ± 0.2	CNS+
13	14.3 ± 0.4	CNS+
15	9.71 ± 0.52	CNS+
17	13.2 ± 0.7	CNS+
28	8.89 ± 0.37	CNS+

[a] Data are the mean ± SEM of three independent experiments; [b] *Pe* (10^{-6} cm s^{-1}) > 4.5 for high BBB permeation (CNS+), *Pe* (10^{-6} cm s^{-1}) < 1.85 for low BBB permeation (CNS−), and 4.04 > *Pe* (10^{-6} cm s^{-1}) > 1.85 for uncertain BBB permeation (CNS±).

2.8. Acute toxicity test *in vivo*

According to the results of *in silicon* prediction, most of the compounds showed a probability of hepatotoxicity. Therefore, it is necessary to test the *in vivo* toxicity of the most promising compound **13**. The procedure for acute toxicity study followed similar protocols from the reported studies [36, 37]. After administration of the compound **13** (2,000 mg/kg), mice were monitored continuously for the first 4 h for any abnormal behavior and mortality changes, intermittently for the next 24 h, and occasionally thereafter for 14 days to monitor the onset of any delayed effects. During the experimental period, no acute toxicity, such as mortality, or significant abnormal

changes in water or food consumption or body weight reduction were observed (**Fig 8**). Furthermore, all mice were sacrificed on the 14th day after drug administration. This indicated that **13** was nontoxic and tolerated at doses up to 2,000 mg/kg.

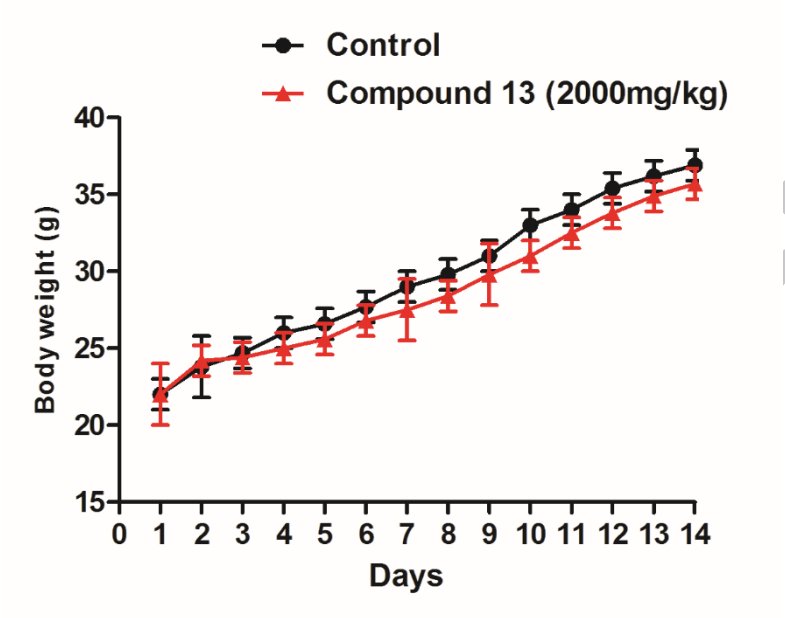

Fig 8.

2.9. Statistical analysis

Statistical analyses were performed with one-way ANOVA test followed by a post hoc analysis (Tukey's multiple comparison test) using GraphPad Prism 5 Software for Windows (GraphPad Software, Inc., San Diego, CA, USA). All values were presented as mean ± standard error of the mean (mean ± SEM) for each group. $P < 0.05$ was considered statistical significant.

3. Conclusions

In conclusion, this study showed that most of the representative benzyloxy substituted derivatives **5-8**, **12-17**, **25**, **28** and **31** not only possessed selective and potent MAO-B inhibitory activities, but also exhibited neuroprotective properties in 6-OHDA- and rotenone-treated PC12 cells. Additionally, the selected compounds displayed no significant cytotoxicity, fine oral absorption and BBB permeability when evaluated for ADMET properties *in silico*. Moreover, the most promising compound **13** exhibited neuroprotective effects via reducing intracellular ROS and preventing neurotoxins-induced apoptosis. Furthermore, **13** showed good BBB permeability and

low toxicity according to *in vitro* BBB prediction and *in vivo* acute toxicity test. Based on the results, compound **13** and other benzyloxy substituted MAO-B inhibitors could be used for the further development of promising drug candidates for the therapy of Parkinson's disease.

4. Methods

4.1. Chemistry

All common reagents and solvents were obtained from commercial suppliers and used without further purification. Reaction progress was monitored using analytical thin layer chromatography (TLC) on precoated silica gel GF254 plates (Qingdao Haiyang Chemical Plant, Qingdao, China) plates and the spots were detected under UV light (254 nm). Column chromatography was performed on silica gel (90-150 μm; Qingdao Marine Chemical Inc.) Melting points were measured on an XT-4 micromelting point instrument and uncorrected. NMR spectra were measured on a Bruker ACF-500 spectrometer at 25 °C and referenced to TMS. Chemical shifts are reported in ppm (δ) using the residual solvent line as internal standard. Mass spectra were obtained on a MS Agilent 1100 Series LC/MSD Trap mass spectrometer (ESI-MS) and a Mariner ESI-TOF spectrometer (HRESI-MS), respectively.

4.1.1. General procedure for the preparation of the benzyloxy substituted derivatives (1-31)

The procedures for the preparation of the key intermediates (**S1**-**4**) were summarized in supporting information. The starting material (1.0 mmol) was suspended in acetonitrile (20 mL) containing K_2CO_3 (2.0 mmol). The reaction was treated with an appropriately substituted arylalkyl bromide (1.2 mmol) and heated under reflux for 8 h. The reaction progress was monitored using *silica gel* TLC with Petroleum ether/EtOAc as mobile phase. Upon completion, the acetonitrile was evaporated *in vacuo* and the mixture was then poured into water, which was extracted with 3 × 50 mL of EtOAc, washed with brine, dried over anhydrous Na_2SO_4 and purified by chromatography (PE/EA, 50:1, 20:1, 10:1) on *silica gel.*

*1-(4-((4-fluorobenzyl)oxy)phenyl)ethanone (**1**).* Yield 83%, white solid, m.p. 75-77 °C;

Purity 97.5%; ^{1}H NMR (500 MHz, DMSO-d6) δ 7.95 (d, J = 8.8 Hz, 2H), 7.54 (dd, J = 8.4, 5.7 Hz, 2H), 7.25 (t, J = 8.8 Hz, 2H), 7.13 (d, J = 8.8 Hz, 2H), 5.21 (s, 2H), 2.53 (s, 3H); ^{13}C NMR (125 MHz, DMSO-d6) δ 196.72, 162.56, 161.39, 133.26, 130.93, 130.93, 130.68, 130.54, 130.48, 115.87, 115.70, 115.15, 115.15, 69.29, 26.84. ESI-MS *m/z*: 244.9 $[M+H]^+$; HRMS (ESI) *m/z* 245.0970 $[M+H]^+$ (calcd for 245.0972, $C_{15}H_{14}FO_2$).

*1-(4-((3-chlorobenzyl)oxy)phenyl)ethanone (**2**)*. Yield 89%, white solid, m.p. 79-81 °C; Purity 98.6%; ^{1}H NMR (500 MHz, DMSO-d6) δ 7.96 (d, J = 8.8 Hz, 2H), 7.55 (s, 1H), 7.49 - 7.39 (m, 3H), 7.14 (d, J = 8.8 Hz, 2H), 5.25 (s, 2H), 2.53 (s, 3H); ESI-MS *m/z*: 260.9 $[M+H]^+$; ^{13}C NMR (125 MHz, DMSO-d6) δ 196.73, 162.39, 139.61, 133.67, 130.95, 130.95, 130.89, 130.78, 128.39, 127.84, 126.69, 115.16, 115.16, 69.05, 26.85. HRMS (ESI) *m/z* 261.0679 $[M+H]^+$ (calcd for 261.0677, $C_{15}H_{14}ClO_2$).

*1-(3-((4-chlorobenzyl)oxy)phenyl)ethanone (**3**)*. Yield 82%, light yellow oil; Purity 99.3%; ^{1}H NMR (500 MHz, DMSO-d6) δ 7.59 (d, J = 7.7 Hz, 1H), 7.55 (d, J = 2.0 Hz, 1H), 7.54 - 7.43 (m, 5H), 7.30 (dd, J = 8.0, 2.2 Hz, 1H), 5.20 (s, 2H), 2.59 (s, 3H); ^{13}C NMR (125 MHz, DMSO-d6) δ 198.11, 158.83, 138.83, 136.37, 132.98, 130.39, 129.97, 129.97, 128.95, 128.95, 121.55, 120.41, 114.28, 69.13, 27.29. ESI-MS *m/z*: 260.9 $[M+H]^+$; HRMS (ESI) *m/z* 261.0676 $[M+H]^+$ (calcd for 261.0677, $C_{15}H_{14}ClO_2$).

*1-(3-((4-bromobenzyl)oxy)phenyl)ethanone (**4**)*. Yield 90%, light yellow oil; Purity 99.7%; ^{1}H NMR (500 MHz, DMSO-d6) δ 7.60 (dd, J = 14.3, 8.0 Hz, 3H), 7.54 (s, 1H), 7.51 - 7.40 (m, 3H), 7.30 (dd, J = 8.2, 1.9 Hz, 1H), 5.19 (s, 2H), 2.59 (s, 3H); ^{13}C NMR (125 MHz, DMSO-d6) δ 198.10, 158.81, 138.83, 136.80, 131.87, 131.87, 130.39, 130.27, 130.27, 121.56, 121.49, 120.41, 114.28, 69.16, 27.29. ESI-MS *m/z*: 306.9 $[M+H]^+$; HRMS (ESI) *m/z* 326.9990 $[M+Na]^+$ (calcd for 326.9991, $C_{15}H_{13}BrNaO_2$).

*1-(4-((3-fluorobenzyl)oxy)-2-hydroxyphenyl)ethanone (**5**)*. Yield 89%, white solid, m.p. 103-104 °C; Purity 98.5%; ^{1}H NMR (500 MHz, DMSO-d6) δ 12.61 (s, 1H), 7.88 (d, J = 8.9 Hz, 1H), 7.54 – 7.39 (m, 1H), 7.30 (dd, J = 7.8, 4.7 Hz, 2H), 7.19 (td, J = 8.6, 1.9 Hz, 1H), 6.64 (dd, J = 8.9, 2.4 Hz, 1H), 6.58 (d, J = 2.4 Hz, 1H), 5.24 (s, 2H),

2.59 (s, 3H); ^{13}C NMR (125 MHz, DMSO-d6) δ 202.37, 165.04, 164.75, 163.75, 162.12, 138.41, 138.36, 132.39, 130.28, 130.23, 122.73, 122.71, 115.21, 115.07, 114.29, 114.19, 114.15, 108.02, 101.83, 101.81, 69.27, 69.25, 26.51. ESI-MS *m/z*: 260.9 $[M+H]^+$; HRMS (ESI) *m/z* 261.0922 $[M+H]^+$ (calcd for 261.0921, $C_{15}H_{14}FO_3$).

*1-(4-((4-fluorobenzyl)oxy)-2-hydroxyphenyl)ethanone (**6**)*. Yield 85%, white solid, m.p. 111-112 °C; Purity 98.5%; ^{1}H NMR (500 MHz, DMSO-d6) δ 12.62 (s, 1H), 7.87 (d, J = 8.9 Hz, 1H), 7.53 (dd, J = 8.4, 5.7 Hz, 2H), 7.25 (t, J = 8.9 Hz, 2H), 6.62 (dd, J = 8.9, 2.4 Hz, 1H), 6.58 (d, J = 2.4 Hz, 1H), 5.19 (s, 2H), 2.58 (s, 3H); ^{13}C NMR (125 MHz, DMSO-d6) δ 201.19, 165.13, 164.92, 163.45, 161.81, 132.36, 131.60, 131.58, 129.45, 129.40, 115.70, 115.56, 114.12, 108.07, 101.78, 101.77, 69.49, 26.34. ESI-MS *m/z*: 260.9 $[M+H]^+$; HRMS (ESI) *m/z* 261.0916 $[M+H]^+$ (calcd for 261.0922, $C_{15}H_{14}FO_3$).

*1-(4-((3-chlorobenzyl)oxy)-2-hydroxyphenyl)ethanone (**7**)*. Yield 83%, white solid, m.p. 128-129 °C; Purity 99.6%; ^{1}H NMR (500 MHz, DMSO-d6) δ 12.61 (s, 1H), 7.88 (d, J = 8.9 Hz, 1H), 7.54 (s, 1H), 7.50 – 7.34 (m, 3H), 6.64 (dd, J = 8.9, 2.4 Hz, 1H), 6.58 (d, J = 2.4 Hz, 1H), 5.24 (s, 2H), 2.59 (s, 3H); ^{13}C NMR (125 MHz, DMSO-d6) δ 202.63, 165.11, 164.74, 137.88, 134.61, 132.40, 129.96, 128.41, 127.41, 125.35, 114.22, 108.02, 101.82, 69.24, 26.25. ESI-MS *m/z*: 274.9 $[M-H]^-$; HRMS (ESI) *m/z* 275.0479 $[M-H]^-$ (calcd for 275.0480, $C_{15}H_{12}ClO_3$).

*1-(4-((4-chlorobenzyl)oxy)-2-hydroxyphenyl)ethanone (**8**)*. Yield 88%, white solid, m.p. 102-103 °C; Purity 100%;^{1}H NMR (500 MHz, DMSO-d6) δ 12.61 (s, 1H), 7.87 (d, J = 8.9 Hz, 1H), 7.58 – 7.39 (m, 4H), 6.62 (dd, J = 8.9, 2.4 Hz, 1H), 6.57 (d, J = 2.4 Hz, 1H), 5.22 (s, 2H), 2.58 (s, 3H); ^{13}C NMR (125 MHz, DMSO-d6) δ 202.60, 165.10, 164.80, 134.32, 134.11, 132.37, 128.86, 128.79, 114.16, 108.01, 101.80, 69.34, 26.24. ESI-MS *m/z*: 274.9 $[M+H]^+$; HRMS (ESI) *m/z* 275.0482 $[M-H]^-$ (calcd for 275.0480, $C_{15}H_{12}ClO_3$).

*1-(2-fluoro-4-((3-fluorobenzyl)oxy)phenyl)ethanone (**9**)*. Yield 93%, light yellow solid, m.p. 104-105 °C; Purity 99.4%; ^{1}H NMR (500 MHz, DMSO-d6) δ 7.83 (t, J = 8.9 Hz, 1H), 7.48 (dd, J = 14.2, 7.7 Hz, 1H), 7.32 (d, J = 7.8 Hz, 2H), 7.20 (dd, J = 9.1, 7.2

Hz, 1H), 7.05 (dd, *J* = 13.5, 2.2 Hz, 1H), 6.99 (dd, *J* = 8.8, 2.3 Hz, 1H), 5.27 (s, 2H), 2.53 (s, 3H); ^{13}C NMR (500 MHz, DMSO-d6) δ 193.5, 163.8, 163.1, 161.1, 138.9, 131.7, 130.5, 123.6, 118.4, 114.9, 114.2, 111.7, 102.9, 69.1, 30.6. ESI-MS *m/z*: 262.9 $[M+H]^+$; HRMS (ESI) *m/z* 263.0879 $[M+H]^+$ (calcd for 263.0878, $C_{15}H_{13}F_2O_2$).

1-(2-fluoro-4-((4-fluorobenzyl)oxy)phenyl)ethanone ***(10)***. Yield 87%, light yellow solid, m.p. 69-71 °C; Purity 99.2%; ^{1}H NMR (500 MHz, DMSO-d6) δ 7.83 (t, *J* = 8.9 Hz, 1H), 7.54 (dd, *J* = 8.3, 5.7 Hz, 2H), 7.25 (t, *J* = 8.8 Hz, 2H), 7.04 (dd, *J* = 13.6, 1.1 Hz, 1H), 6.98 (dd, *J* = 8.8, 2.1 Hz, 1H), 5.22 (s, 2H), 2.53 (s, 3H); ^{13}C NMR (125 MHz, DMSO-d_6) δ 193.5, 163.8, 162.8, 160.9, 132.2, 131.7, 130.2, 130.2, 118.3, 115.4, 115.4, 111.7, 102.8, 69.3, 30.6. ESI-MS *m/z*: 262.9 $[M+H]^+$; HRMS (ESI) *m/z* 263.0877 $[M+H]^+$ (calcd for 263.0878, $C_{15}H_{13}F_2O_2$).

1-(2-fluoro-4-((3-chlorobenzyl)oxy)phenyl)ethanone ***(11)***. Yield 93%, light yellow solid, m.p. 70-72 °C; Purity 99.9%; ^{1}H NMR (500 MHz, DMSO-d6) δ 7.83 (t, *J* = 8.9 Hz, 1H), 7.56 (s, 1H), 7.51 – 7.38 (m, 3H), 7.05 (d, *J* = 13.5 Hz, 1H), 7.00 (dd, *J* = 8.8, 2.0 Hz, 1H), 5.26 (s, 2H), 2.53 (s, 3H); ^{13}C NMR (125 MHz, DMSO-d_6) δ 193.6, 163.8, 161.8, 138.5, 133.1, 131.7, 130.4, 128.0, 127.4, 126.3, 118.4, 111.7, 102.9, 69.0, 30.6. ESI-MS *m/z*: 278.9 $[M+H]^+$; HRMS (ESI) *m/z* 301.0400 $[M+Na]^+$ (calcd for 301.0402, $C_{15}H_{12}ClFNaO_2$).

1-(2-fluoro-4-((4-chlorobenzyl)oxy)phenyl)ethanone ***(12)***. Yield 85%, light yellow solid, m.p. 74-75 °C; Purity 100%; ^{1}H NMR (500 MHz, DMSO-d6) δ 7.83 (t, *J* = 8.9 Hz, 1H), 7.57 – 7.42 (m, 4H), 7.04 (dd, *J* = 13.5, 1.6 Hz, 1H), 6.98 (dd, *J* = 8.8, 1.9 Hz, 1H), 5.24 (s, 2H), 2.53 (s, 3H); ^{13}C NMR (125 MHz, DMSO-d_6) δ 193.5, 163.8, 161.8, 135.0, 132.7, 131.7, 129.6, 129.6, 128.4, 128.4, 118.3, 111.7, 102.9, 69.1, 30.7. ESI-MS *m/z*: 278.9 $[M+H]^+$; HRMS (ESI) *m/z* 301.0403 $[M+Na]^+$ (calcd for 301.0402, $C_{15}H_{12}ClFNaO_2$).

7-((4-Fluorobenzyl)oxy)chroman-4-one ***(13)***. Yield 91%, colorless solid, m.p. 125-127 °C; Purity 99.9%; ^{1}H NMR (500 MHz, DMSO-d6) δ 7.69 (d, *J* = 8.8 Hz, 1H), 7.50 (dd, *J* = 8.5, 5.6 Hz, 2H), 7.23 (t, *J* = 8.8 Hz, 2H), 6.70 (dd, *J* = 8.8, 2.3 Hz, 1H), 6.63 (d, *J* = 2.3 Hz, 1H), 5.16 (s, 2H), 4.51 (t, *J* = 6.4 Hz, 2H), 2.71 (t, *J* = 6.4 Hz, 2H);

^{13}C NMR (125 MHz, DMSO-d6) δ 189.86, 164.25, 163.27, 162.79, 132.47, 132.45, 130.01, 129.95, 128.12, 115.33, 115.16, 110.09, 101.78, 68.93, 67.04, 36.82. ESI-MS *m/z*: 272.9 $[M+H]^+$; HRMS (ESI) m/z 567.1586 $[2M+Na]^+$ (calcd for 567.1590, $C_{32}H_{26}NaO_6F_2$).

7-((4-Chlorobenzyl)oxy)chroman-4-one ***(14)***. Yield 89%, colorless solid, m.p. 139-140 °C; Purity 99.6%; ^{1}H NMR (500 MHz, DMSO-d6) δ 7.69 (d, J = 8.8 Hz, 1H), 7.47 (s, 4H), 6.70 (dd, J = 8.8, 2.4 Hz, 1H), 6.62 (d, J = 2.4 Hz, 1H), 5.18 (s, 2H), 4.50 (t, J = 6.4 Hz, 2H), 2.70 (t, J = 6.4 Hz, 2H); ^{13}C NMR (125 MHz, DMSO-d6) δ 190.44, 164.71, 163.82, 135.86, 133.15, 130.05, 130.05, 129.01, 129.01, 128.71, 115.62, 110.66, 102.38, 69.33, 67.61, 37.37. ESI-MS *m/z*: 288.9 $[M+H]^+$; HRMS (ESI) m/z 311.0446 $[M+Na]^+$ (calcd for 311.0445, $C_{16}H_{13}ClNaO_3$).

7-((4-fluorobenzyl)oxy)-2,2-dimethylchroman-4-one ***(15)***. Yield 87%, yellow solid, m.p. 91-92 °C; Purity 98.6%; ^{1}H NMR (500 MHz, DMSO-d6) δ 7.66 (d, J = 8.7 Hz, 1H), 7.50 (dd, J = 8.5, 5.6 Hz, 2H), 7.23 (t, J = 8.8 Hz, 2H), 6.66 (dd, J = 8.8, 2.3 Hz, 1H), 6.58 (d, J = 2.3 Hz, 1H), 5.15 (s, 2H), 2.71 (s, 2H), 1.39 (s, 6H); ^{13}C NMR (125 MHz, DMSO-d6) δ 190.78, 165.18, 163.48, 161.88, 133.09, 130.61, 130.54, 128.10, 115.89, 115.72, 114.29, 110.12, 102.65, 80.16, 69.47, 48.26, 26.62, 26.62. ESI-MS *m/z*: 300.9 $[M+H]^+$; HRMS (ESI) m/z 623.2210 $[2M+Na]^+$ (calcd for 623.2216, $C_{36}H_{34}F_2NaO_6$).

7-((4-chlorobenzyl)oxy)-2,2-dimethylchroman-4-one ***(16)***. Yield 85%, colorless solid, m.p. 130-131 °C; Purity 99.5%; ^{1}H NMR (500 MHz, DMSO-d6) δ 7.66 (d, J = 8.7 Hz, 1H), 7.46 (s, 4H), 6.66 (dd, J = 8.7, 2.3 Hz, 1H), 6.57 (d, J = 2.3 Hz, 1H), 5.17 (s, 2H), 2.70 (s, 2H), 1.38 (s, 6H); ^{13}C NMR (125 MHz, DMSO-d6) δ 190.79, 165.08, 161.86, 135.91, 133.14, 130.07, 130.07, 129.00, 129.00, 128.12, 114.40, 110.13, 102.67, 80.18, 69.31, 48.24, 26.62, 26.62. ESI-MS *m/z*: 317.1 $[M+H]^+$; HRMS (ESI) m/z 655.1621 $[2M+Na]^+$ (calcd for 655.1625, $C_{36}H_{34}Cl_2NaO_6$).

6-((4-fluorobenzyl)oxy)-3,4-dihydronaphthalen-1(2H)-one ***(17)***. Yield 87%, yellow solid, m.p. 83-85 °C; Purity 98.8%; ^{1}H NMR (500 MHz, DMSO-d6) δ 7.85 (d, J = 9.4 Hz, 1H), 7.53 (dd, J = 8.1, 5.8 Hz, 2H), 7.25 (t, J = 8.8 Hz, 2H), 6.98 (d, J = 5.4 Hz,

2H), 5.19 (s, 2H), 2.92 (t, *J* = 5.9 Hz, 2H), 2.58 – 2.53 (m, 2H), 2.14 – 1.92 (m, 2H); ^{13}C NMR (125 MHz, DMSO-d6) *δ* 196.48, 162.57, 147.62, 133.25, 133.23, 130.53, 130.46, 129.18, 126.48, 115.86, 115.69, 114.31, 114.10, 69.23, 38.86, 29.80, 23.42. ESI-MS *m/z*: 271.0 $[M+H]^+$; HRMS (ESI) m/z 293.0947 $[M+Na]^+$ (calcd for 293.0948, $C_{17}H_{15}FNaO_2$).

6-((4-chlorobenzyl)oxy)-3,4-dihydronaphthalen-1(2H)-one ***(18)***. Yield 81%, yellow solid, m.p. 97-99 °C; Purity 99.0%; ^{1}H NMR (500 MHz, DMSO-d6) *δ* 7.93 – 7.77 (m, 1H), 7.62 - 7.40 (m, 4H), 6.98 (d, *J* = 1.8 Hz, 2H), 5.21 (s, 2H), 2.92 (t, *J* = 5.8 Hz, 2H), 2.58 - 2.53 (m, 2H), 2.11 - 1.89 (m, 2H); ^{13}C NMR (125 MHz, DMSO-d6) *δ* 196.49, 162.48, 147.63, 136.08, 133.08, 130.01, 129.20, 128.97, 126.54, 114.32, 114.13, 69.09, 38.86, 29.80, 23.42. ESI-MS *m/z*: 287.0 $[M+H]^+$; HRMS (ESI) m/z 309.0650 $[M+Na]^+$ (calcd for 309.0653, $C_{17}H_{15}ClNaO_2$).

7-((3-chlorobenzyl)oxy)-4H-chromen-4-one ***(19)***. Yield 81%, white solid, m.p. 136-138 °C; Purity 96.5%; ^{1}H NMR (500 MHz, DMSO-d6) *δ* 8.24 (d, *J* = 6.0 Hz, 1H), 7.98 (d, *J* = 8.9 Hz, 1H), 7.58 (s, 1H), 7.46 (dd, *J* = 12.6, 5.4 Hz, 3H), 7.25 (d, *J* = 2.1 Hz, 1H), 7.17 (dd, *J* = 8.9, 2.2 Hz, 1H), 6.29 (d, *J* = 6.0 Hz, 1H), 5.30 (s, 2H); ^{13}C NMR (125 MHz, DMSO-d6) *δ* 176.08, 162.98, 158.13, 156.95, 139.16, 133.69, 130.94, 128.54, 128.01, 127.01, 126.85, 118.87, 115.53, 112.69, 102.44, 69.58. ESI-MS *m/z*: 286.9 $[M+H]^+$; HRMS (ESI) m/z 309.0287 $[M+Na]^+$ (calcd for 309.0289, $C_{16}H_{11}ClNaO_3$).

7-((4-fluorobenzyl)oxy)-4H-chromen-4-one ***(20)***. Yield 86%, white solid, m.p. 121-123 °C; Purity 99.0%; ^{1}H NMR (500 MHz, DMSO-d6) *δ* 8.23 (d, *J* = 6.0 Hz, 1H), 7.97 (d, *J* = 8.9 Hz, 1H), 7.56 (dd, *J* = 8.0, 5.9 Hz, 2H), 7.34 – 7.21 (m, 3H), 7.15 (dd, *J* = 8.9, 1.9 Hz, 1H), 6.29 (d, *J* = 6.0 Hz, 1H), 5.26 (s, 2H); ^{13}C NMR (125 MHz, DMSO-d6) *δ* 176.09, 163.13, 161.46, 158.16, 156.93, 132.85, 130.75, 130.68, 126.95, 118.77, 115.93, 115.76, 115.57, 112.68, 102.37, 69.84. ESI-MS *m/z*: 270.9 $[M+H]^+$; HRMS (ESI) m/z 293.0583 $[M+Na]^+$ (calcd for 293.0584, $C_6H_{11}FNaO_3$).

7-((4-(trifluoromethyl)benzyl)oxy)-4H-chromen-4-one ***(21)***. Yield 80%, white solid, m.p. 159-161 °C; Purity 99.9%; ^{1}H NMR (500 MHz, DMSO-d6) *δ* 8.24 (d, *J* = 6.0 Hz,

1H), 7.99 (d, *J* = 8.9 Hz, 1H), 7.80 (d, *J* = 8.1 Hz, 2H), 7.73 (d, *J* = 8.1 Hz, 2H), 7.26 (d, *J* = 2.2 Hz, 1H), 7.18 (dd, *J* = 8.9, 2.3 Hz, 1H), 6.30 (d, *J* = 6.0 Hz, 1H), 5.41 (s, 2H); ^{13}C NMR (125 MHz, DMSO-d6) δ 176.08, 162.93, 158.14, 156.97, 141.47, 128.69, 127.05, 125.92, 125.89, 123.58, 121.86, 118.92, 115.53, 112.70, 102.48, 69.59. ESI-MS *m/z*: 321.0 $[M+H]^+$; HRMS (ESI) m/z 343.0553 $[M+Na]^+$ (calcd for 343.0552, $C_{17}H_{11}F_3NaO_3$).

6-((4-fluorobenzyl)oxy)-4H-chromen-4-one ***(22)***. Yield 45%, colorless solid, m.p. 139-141 °C; Purity 99.8%; ^{1}H NMR (500 MHz, DMSO-d6) δ 7.83 (d, *J* = 5.9 Hz, 1H), 7.67 - 7.59 (m, 1H), 7.46 - 7.37 (m, 3H), 7.30 (dt, *J* = 9.2, 2.2 Hz, 1H), 7.07 (t, *J* = 8.4 Hz, 2H), 6.31 (d, *J* = 6.0 Hz, 1H), 5.08 (s, 2H); ^{13}C NMR (125 MHz, DMSO-d6) δ 176.83, 163.14, 158.09, 154.78, 138.26, 132.53, 128.39, 127.62, 127.17, 118.83, 114.99, 112.88, 101.39, 70.15. ESI-MS m/z: 270.9 $[M+H]^+$; HRMS (ESI) m/z 271.0694 $[M+H]^+$ (calcd for 271.0692, $C_{16}H_{12}FO_3$).

6-((4-chlorobenzyl)oxy)-4H-chromen-4-one ***(23)***. Yield 65%, colorless solid, m.p. 169-171 °C; Purity 99.7%; ^{1}H NMR (500 MHz, DMSO-d6) δ 7.82 (d, *J* = 5.9 Hz, 1H), 7.68 - 7.59 (m, 1H), 7.48 - 7.26 (m, 6H), 6.35 - 6.24 (m, 1H), 5.08 (s, 2H); ^{13}C NMR (125 MHz, DMSO-d6) δ 175.94, 162.46, 157.64, 156.58, 135.55, 131.43, 130.04, 126.48, 121.32, 118.28, 115.12, 112.19, 101.81, 69.56. ESI-MS *m/z*: 286.9 $[M+H]^+$; HRMS (ESI) m/z 287.0395 $[M+H]^+$ (calcd for 287.0397, $C_{16}H_{12}ClO_3$).

5-((4-fluorobenzyl)oxy)isobenzofuran-1(3H)-one ***(24)***. Yield 85%, colorless solid, m.p. 133-134 °C; Purity 99.8%; ^{1}H NMR (500 MHz, DMSO-d6) δ 7.55 (dd, *J* = 11.4, 5.0 Hz, 3H), 7.26 (t, *J* = 8.9 Hz, 2H), 6.93 (d, *J* = 1.9 Hz, 1H), 6.79 (dd, *J* = 8.6, 2.0 Hz, 1H), 5.23 (s, 2H), 4.79 (s, 2H); ^{13}C NMR (125 MHz, DMSO-d6) δ 171.08, 159.49, 139.32, 134.53, 134.21, 128.99, 128.87, 127.15, 123.71, 123.12, 108.71, 69.72, 69.53. ESI-MS *m/z*: 259.0 $[M+H]^+$; HRMS (ESI) m/z 281.0586 $[M+Na]^+$ (calcd for 281.0584, $C_{15}H_{11}FNaO_3$).

5-((4-chlorobenzyl)oxy)isobenzofuran-1(3H)-one ***(25)***. Yield 75%, colorless solid, m.p. 130-131 °C; Purity 99.4%; ^{1}H NMR (500 MHz, DMSO-d6) δ 7.56 (d, *J* = 8.6 Hz, 1H), 7.51 (q, *J* = 8.6 Hz, 4H), 6.92 (d, *J* = 1.6 Hz, 1H), 6.80 (dd, *J* = 8.6, 1.9 Hz, 1H),

5.26 (s, 2H), 4.79 (s, 2H); ^{13}C NMR (125 MHz, DMSO-d6) δ 171.13, 159.55, 139.27, 131.86, 129.49, 127.12, 123.76, 123.14, 115.78, 115.67, 108.66, 69.85, 69.52. ESI-MS *m/z*: 274.9 $[M+H]^+$; HRMS (ESI) m/z 297.0286 $[M+Na]^+$ (calcd for 297.0289, $C_{15}H_{11}ClNaO_3$).

*5-((4-(trifluoromethyl)benzyl)oxy)isobenzofuran-1(3H)-one (**26**).* Yield 85%, colorless solid, m.p. 127-128 °C; Purity 98.7%; ^{1}H NMR (500 MHz, DMSO-d6) δ 7.76 (dd, *J* = 45.4, 7.9 Hz, 4H), 7.58 (d, *J* = 8.6 Hz, 1H), 6.94 (s, 1H), 6.88 – 6.75 (m, 1H), 5.38 (s, 2H), 4.79 (s, 2H); ^{13}C NMR (125 MHz, DMSO-d6) δ 171.03, 159.35, 140.09, 139.40, 130.38, 127.45, 127.27, 125.73, 124.95, 123.62, 123.21, 108.65, 69.58, 69.54. ESI-MS *m/z*: 309.0 $[M+H]^+$; HRMS (ESI) m/z 331.0556 $[M+Na]^+$ (calcd for 331.0552, $C_{16}H_{11}F_3NaO_3$).

*7-((3-chlorobenzyl)oxy)-3,4-dihydroquinolin-2(1H)-one (**27**).* Yield 68%, white solid, m.p. 158-160 °C; Purity 98.8%; ^{1}H NMR (500 MHz, DMSO-d6) δ 10.01 (s, 1H), 7.64 (s, 1H), 7.54 (d, *J* = 7.9 Hz, 1H), 7.45 (d, *J* = 7.6 Hz, 1H), 7.37 (t, *J* = 7.8 Hz, 1H), 7.08 (d, *J* = 8.2 Hz, 1H), 6.58 (dd, *J* = 8.2, 2.1 Hz, 1H), 6.53 (d, *J* = 1.9 Hz, 1H), 5.07 (s, 2H), 2.80 (t, *J* = 7.5 Hz, 2H), 2.43 (t, *J* = 7.5 Hz, 2H); ^{13}C NMR (125 MHz, DMSO-d6) δ 170.72, 157.81, 140.47, 139.79, 131.12, 131.09, 130.55, 128.93, 126.95, 122.16, 116.59, 108.35, 102.65, 68.77, 31.19, 24.52. ESI-MS *m/z*: 288.0 $[M+H]^+$; HRMS (ESI) m/z 288.0785 $[M+H]^+$ (calcd for 288.0786, $C_{16}H_{15}ClNO_2$).

*7-((3-bromobenzyl)oxy)-3,4-dihydroquinolin-2(1H)-one (**28**).* Yield 76%, white solid, m.p. 125-127 °C; Purity 98.7%; ^{1}H NMR (500 MHz, DMSO-d6) δ 10.01 (s, 1H), 7.50 (s, 1H), 7.47 – 7.36 (m, 3H), 7.08 (d, *J* = 8.3 Hz, 1H), 6.58 (dd, *J* = 8.2, 2.3 Hz, 1H), 6.53 (d, *J* = 2.2 Hz, 1H), 5.07 (s, 2H), 2.80 (t, *J* = 7.5 Hz, 2H), 2.43 (t, *J* = 7.5 Hz, 2H); ^{13}C NMR (125 MHz, DMSO-d6) δ 170.73, 157.81, 140.22, 139.79, 133.60, 130.83, 128.93, 128.18, 127.67, 126.55, 116.59, 108.35, 102.65, 68.83, 31.19, 24.51. ESI-MS *m/z*: 332.0 $[M+H]^+$; HRMS (ESI) m/z 332.0280 $[M+H]^+$ (calcd for 332.0281, $C_{16}H_{15}BrNO_2$).

*7-((4-fluorobenzyl)oxy)-3,4-dimethyl-2H-chromen-2-one (**29**).* Yield 81%, light yellow solid, m.p. 139-141 °C; Purity 99.8%; ^{1}H NMR (500 MHz, DMSO-d6) δ 7.68

(d, *J* = 8.5 Hz, 1H), 7.18 (t, *J* = 7.7 Hz, 1H), 7.00 – 6.96 (m, 2H), 6.87 – 6.83 (m, 2H), 6.70 (dd, *J* = 8.5, 1.6 Hz, 1H), 5.15 (s, 2H), 2.34 (s, 3H), 2.06 (s, 3H); ^{13}C NMR (125 MHz, DMSO-d6) δ 163.78, 161.29, 160.74, 156.49, 147.18, 142.56, 130.57, 129.73, 129.07, 125.82, 119.57, 115.46, 113.54, 104.09, 69.87, 20.13, 18.50. ESI-MS *m/z*: 299.0 $[M+H]^+$; HRMS (ESI) m/z 321.0895 $[M+Na]^+$ (calcd for 321.0897, $C_{18}H_{15}FNaO_3$).

7-((4-chlorobenzyl)oxy)-3,4-dimethyl-2H-chromen-2-one ***(30)***. Yield 75%, light yellow solid, m.p. 135-137 °C; Purity 99.6%; ^{1}H NMR (500 MHz, DMSO-d6) δ 7.69 (d, *J* = 8.9 Hz, 1H), 7.42 (d, *J* = 8.1 Hz, 2H), 7.29 (d, *J* = 8.1 Hz, 2H), 7.11 – 6.99 (m, 1H), 6.94 (dd, *J* = 8.9 Hz, *J* = 2.8 Hz, 1H), 5.13 (s, 2H), 2.37 (s, 3H), 2.06 (s, 3H); ^{13}C NMR (125 MHz, DMSO-d6) δ 166.52, 160.31, 154.82, 147.23, 140.25, 134.87, 130.79, 133.24, 130.18, 129.73, 129.07, 125.82, 119.57, 113.54, 104.12, 70.81, 20.09, 18.45. ESI-MS *m/z*: 315.0 $[M+H]^+$; HRMS (ESI) m/z 337.0601 $[M+Na]^+$ (calcd for 337.0602, $C_{18}H_{15}ClNaO_3$).

7-((3,4-difluorobenzyl)oxy)-3,4-dimethyl-2H-chromen-2-one ***(31)***. Yield 73%, light yellow solid, m.p. 152-155 °C; Purity 98.7%; ^{1}H NMR (500 MHz, DMSO-d6) δ 7.48 (d, *J* = 8.8 Hz, 1H), 7.09 – 7.03 (m, 2H), 6.91 – 6.88 (m, 1H), 6.88 (dd, *J* = 8.9, 2.8 Hz, 1H), 6.81 (d, *J* = 2.3 Hz, 1H), 5.16 (s, 2H), 2.35 (s, 3H), 2.16 (s, 3H); ^{13}C NMR (125 MHz, DMSO-d6) δ 164.67, 160.34, 154.82, 150.11, 147.23, 146.38, 139.75, 134.87, 130.79, 133.24, 130.18, 129.89, 129.12, 125.45, 118.35, 113.65, 104.09, 70.21, 21.13, 18.67. ESI-MS *m/z*: 317.0 $[M+H]^+$; HRMS (ESI) m/z 339.0805 $[M+Na]^+$ (calcd for 339.0806, $C_{36}H_{34}Cl_2NaO_6$).

4.2. MAO inhibition [22-24]

Human MAO-A and MAO-B were purchased from Sigma-Aldrich. Briefly, 0.1 mL of sodium phosphate buffer (0.05 mM, pH 7.4) containing the tested drugs at various concentrations and adequate amounts of recombinant MAO-A or MAO-B required and adjusted to obtain in our experimental conditions the same reaction velocity, i.e., to oxidize (in the control group) the same concentration of substrate: 165 *p*mol of *p*-tyramine/min (MAO-A: 1.1 μg protein; specific activity: 150 nmol of *p*-tyramine

oxidized to *p*-hydroxyphenylacetaldehyde/min/mg protein; MAO-B: 7.5 μg protein; specific activity: 22 nmol of *p*-tyramine transformed/min/mg protein) were incubated for 15 min at 37 °C in a flat-black-bottom 96-well microtest plate placed in a dark fluorimeter chamber. After this incubation period, the reaction was started by adding 200 μM (final concentrations) Amplex Red reagent, 1 U/mL horseradish peroxidase, and 1 mM *p*-tyramine. The production of H_2O_2 and consequently, of resorufin, was quantified at 37 °C in a SpectraMax Paradigm (Molecular Devices, Sunnyvale, CA) muti-mode detection platform reader based on the fluorescence generated (excitation, 545 nm; emission, 590 nm). The specific fluorescence emission was calculated after subtraction of the background activity. The background activity was determined from wells containing all components except the MAO isoforms, which were replaced by a sodium phosphate buffer solution (0.05 mM, pH 7.4). The percent inhibition was calculated by the following expression: (1 - IFi/IFc) × 100% in which IFi and IFc are the fluorescence intensities obtained for MAOs in the presence and absence of inhibitors after subtracting the respective background.

4.3. Cell viability and neuroprotection activity assay

PC12 cells (rat pheochromocytoma) was obtained from the Cell Bank of the Chinese Academy of Sciences (Shanghai, China) and cultured in RPMI-1640 medium containing 10% (v/v) foetal bovine serum, 100 U penicillin/mL and 100 mg streptomycin/mL under 5% CO_2 at 37 °C. The culture media were changed every other day. Cells were subcultured in 96-well plates at a seeding density of 5×10^3 cells/well and allowed to adhere and grow. When cells reached the required confluence, they were placed into serum-free medium and treated with compounds **1-31** (100 μM and 20 μM). Twenty-four hours (and seventy-two hours) later the survival of cells was determined by MTT assay. Briefly, after incubation with 20 μL of MTT at 37 °C for 4 h, living cells containing MTT formazan crystals were solubilized in 150 μL DMSO-D6. The absorbance of each well was measured using a microculture plate reader with a test wavelength of 570 nm and a reference wavelength of 630 nm. Results are expressed as the mean ± SD of three independent

experiments.

PC12 cells were seeded at 5×10^3 cells/well in 96-well plates for neuroprotection activity assay. After 24 h, the medium was removed and replaced with the tested compounds (20 μM) at 37 °C and incubated for another 24 h. Rasagiline was used as the control with the same concentration of 20 μM. Then, the cells were exposed to 6-OHDA (40 μM) and Rotenone (1 μM) respectively, and incubated at 37 °C for 24 h before assayed with MTT. PC12 cells were cultured without test compound or neurotoxins as control groups and the results were expressed by percentage of control. Results are expressed as the mean ± SEM of three independent experiments.

4.4. Annexin V APC/7-AAD double staining to detect apoptosis [29]

Cells growing in the logarithmic phase were trypsinized and seeded into a 6-well plate. The corresponding drug containing medium was added (100, 20 or 4 μg/ml) after the cells were attached to the plate and negative control group was included at the same time. After treatment with the drug for 24 h, 0.25% trypsin (without EDTA) was used to trypsinize and gather the cells. The cells were washed twice with phosphate-buffered saline (PBS) (centrifugation at 2,000 rpm, 5 min), and 2×10^5 cells were collected. The cells were then resuspended in 500 μl of binding buffer. After 5 μl of Annexin V APC was added and mixed well, 5 μl of 7-AAD was added and mixed well. The reaction was performed at room temperature for 5-15 min in the dark, and a flow cytometer (FACSCalibur; Becton-Dickinson, USA) was used to detect apoptosis.

4.5. Hoechst 33258 staining assay [30]

For Hoechst 33258 staining assay, PC12 cells were stained with Hoechst 33258 for 30 min. The cells were plated on the glass slide and covered with cover slip, then observed using a fluorescent inverted microscope (Nikon ti-s, Japan).

4.6. Evaluation of intracellular ROS [31]

The level of intracellular ROS was measured by using the ROS-sensitive dye, 2, 7-dichloro-fluorescein diacetate (DCFH-DA), as a probe. In brief, PC12 cells were seeded in six-well plates at 2×10^5 cells/well, culturing in the presence or absence of

various concentrations of tested samples for additional 24 h, and then washed three times and incubated with final concentration of 10 mM DCFH-DA for 30 min at 37 °C in the dark. After incubation, cells were washed three times and harvested in free-serum medium. The fluorescence of 2, 7-dichlorofluorescein (DCF) was detected by flow cytometry (488 nm excitation and 525 nm emission filters) using BD Accuri C6 flow cytometer (Becton & Dickinson Company, Franklin Lakes, NJ, USA). Data were processed by using cell quest software (Becton & Dickinson Company, Franklin Lakes, NJ).

4.7. *In vitro* BBB permeation assay [33]

Commercial drugs were purchased from Sigma and Alfa Aesar. The porcine brain lipid (PBL) was obtained from Avanti Polar Lipids. The donor microplate (PVDF membrane, pore size 0.45 mm) and the acceptor microplate were both from Millipore. The 96-well UV plate (COSTAR$^{@}$) was from Corning Incorporated. The acceptor 96-well microplate was filled with 300 μL of PBS/EtOH (7:3), and the filter membrane was impregnated with 10 μL of PBL in dodecane (20 mg/mL). Compounds were dissolved in DMSO-D6 at 5 mg/mL and diluted 50-fold in PBS/EtOH (7:3) to achieve a concentration of 100 mg/mL, 200 μL of which was added to the donor wells. The acceptor filter plate was carefully placed on the donor plate to form a sandwich, which was left undisturbed for 16 h at 25 °C. After incubation, the donor plate was carefully removed and the concentration of compound in the acceptor wells was determined using a UV plate reader (Flexsta-tion@ 3). Every sample was analyzed at five wavelengths, in four wells, in at least three independent runs, and the results are given as the mean ± SEM. In each experiment, 9 quality control standards of known BBB permeability were included to validate the analysis set.

4.8. Animals and acute toxicity test [35, 36]

Twenty Kunming mice (20 ± 2 g) were purchased from Laboratory Animal Research Center, Nanjing University (Nanjing, China). Animals were housed in stainless steel cages by sex in a ventilated animal room. Room temperature was maintained at 25 ± 2 °C, relative humidity at 50 ± 10%, and a 12 h light/dark cycle. Distilled water

and sterilized food for mice were available *ad libitum*. They were acclimated to this environment for 5 days prior to dosing. All procedures were approved by the China Pharmaceutical University Animal Care and Use Committee (IACUC) and were in compliance with the National Institute of Health (NIH) guidelines.

Animals were randomly divided into two groups: control group and experimental group (2000 mg/kg, n=10 per group). Before treatment, animals were fasted overnight. Compound **13** was suspended in 0.5% carboxymethyl cellulose sodium (CMC-Na) salt solution and orally administered according to the divided groups. Food and water were provided later. After administration of **13**, the mice were observed continuously for the first 4 h for any abnormal behavior and mortality changes, intermittently for the next 24 h, and occasionally thereafter for 14 days for the onset of any delayed effects. All animals were sacrificed after being anaesthetized by ether on the 14th day after drug administration.

Acknowledgments

The research work was financially supported by the Project of National Natural Sciences Foundation of China (81573313), the Program for Changjiang Scholars and Innovative Research Team in University (PCSIRT-IRT_15R63), and the Priority Academic Program Development of Jiangsu Higher Education Institutions (PAPD).

References

1. Monte, D. A.; DeLanney, L. E.; Irwin, I.; Royland, J. E.; Chan, P.; Jakowec, M. W.; Langston, J. W. *Brain Res*. **1996**, *738*, 53.
2. Finberg, J. P.; Wang, J.; Bankiewich, K.; Harvey-White, J.; Kopin, I. J.; Goldstein, D. S. *J. Neural. Transm. Suppl*. **1998**, *52*, 279.
3. Carlsson, A. *J. Neural. Transm*. **2002**, *109*, 777.
4. Pedrosa, D. J.; Timmermann, L. *Dis. Treat*. **2013**, *9*, 321.
5. Talati, R.; Baker, W. L.; Patel, A. A.; Reinhart, K.; Coleman, C. I. *Int. J. Clin. Pract*. **2009**, *63*, 613.
6. Youdim, M. B. H.; Edmondson, D. E.; Tipton, K. F. *Nat. Rev. Neurosci*. **2006**, *7*, 295.

7. Pålhagen, S.; Heinonen, E. H.; Hägglund, J.; Kaugesaar, T.; Kontants, H.; Mäki-Ikola, O.; Palm, R.; Turunen, J. *Neurology*. **1998**, *51*, 520.

8. Youdim, M. B. H.; Bakhle, Y. S. *Br. J. Pharmacol*. **2006**, *147*, 287.

9. Youdim, M. B. H.; Gross, A. M.; Finberg, J. P. *Br. J. Pharmacol*. **2001**, *132*, 500.

10. Yu, P. H.; Davis, B. A.; Boulton, A. A. *Adv. Exp. Med. Biol.* **1995**, *363*, 17.

11. La Regina, G.; Silvestri, R.; Artico, M.; Lavecchia, A.; Novellino, E.; Befani, O.; Turini P.; Agostinelli, E. *J. Med. Chem*. **2007**, *50*, 922.

12. Huleatt, P. B.; Khoo, M. L.; Chua, Y. Y.; Tan, T. W.; Liew, R. S.; Balogh, B.; Deme, R.; Gölöncsér, F.; Magyar, K.; Sheela, D. P.; Ho, H. K.; Sperlágh, B.; Mátyus, P.; Chai, C. L. *J. Med. Chem*. **2015**, *58*, 1400.

13. Robakis, D.; Fahn, S. *CNS Drugs*. **2015**, *29*, 433.

14. Legoabe, L. J.; Petzer, A.; Petzer, J. P. *Drug. Des. Dev. Ther*. **2015**, *9*, 3635.

15. Lan, J. S.; Xie, S. S.; Huang, M.; Hu, Y. J.; Kong, L. Y.; Wang, X. B. *Med. Chem. Comm.* **2015**, *6*, 1293.

16. Legoabe, L. J.; Petzerand, A.; Petzer, J. P. *Bioorg. Med. Chem. Lett.* **2014**, *24*, 2758.

17. Legoabe, L. J.; Petzer, A.; Petzer, J. P. *Bioorg. Chem*. **2012**, *45*, 1.

18. Legoabe, L. J.; Petzer, A.; Petzer, J. P. *Eur. J. Med. Chem*. **2012**, *49*, 343.

19. Strydom, B.; Bergh, J. J.; Petzer, J. P. *Bioorg. Med. Chem. Lett*. **2013**, *23*, 1269.

20. Meiring, L.; Petzer, J. P. *Bioorg. Med. Chem. Lett*. **2013**, *23*, 5498.

21. Gnerre, C.; Catto, M.; Leonetti, F.; Weber, P.; Carrupt, P. A.; Altomare, C.; Carotti, A.; Testa, B. *J. Med. Chem.* **2000**, *43*, 4747.

22. Novaroli, L.; Reist, M.; Favre, E.; Carotti, A.; Catto, M.; Carrupt, P. A. *Bioorg. Med. Chem.* **2005**, *13*, 6212.

23. Desideri, N.; Fioravanti, R.; Monaco, L. P.; Biava, M.; Yáñez, M.; Ortuso, F.; Alcaro, S. *Eur. J. Med. Chem.* **2013**, *59*, 91.

24. Desideri, N.; Bolasco, A.; Fioravanti, R.; Monaco, L. P.; Orallo, F.; Yáñez, M.; Ortuso, F.; Alcaro, S. *J. Med. Chem*. **2011**, *54*, 2155.

25. Hwang, S. L.; Yen, G. C. *J. Agric. Food. Chem*. **2008**, *56*, 859.

26. Voshavar, C.; Shah, M.; Xu, L.; Dutta, A. K. *Neurotox. Res*. 2015, 28, 302.

27. Cheng, B.; Guo, Y.; Li, C.; Ji, B.; Pan, Y.; Chen, J.; Bai, B. *J. Neurol. Sci*. **2014**, *343*, 115.

28. Zheng, H.; Gal, S.; Weiner, L. M.; Bar-Am, O.; Warshawsky, A.; Fridkin, M.; Youdim, M. B. H. *J. Neurochem*. **2005**, *95*, 68.

29. Zhang, X. Y.; Bai, D. C.; Wu, Y. J.; Li, W.. G.; Liu, N. F. *Can. J. Physiol. Pharmacol*. **2005**, *83*, 309.

30. Janhom, P.; Dharmasaroja, P. *J. Toxicol*. **2015**, *2015*, 1.

31. Gal, S.; Zheng, H.; Fridkin, M.; Youdim, M. B. H. *J. Neurochem*. **2005**, *95*, 79.

32. Grover, J.; Kumar, V.; Singh, V.; Bairwa, K.; Sobhia, M. E.; Jachak, S. M. *Eur. J. Med. Chem*. **2014**, *80*, 47.

33. Lipinski, C. A.; Lombardo, F.; Dominy, B. W.; Feeney, P. J. *Adv. Drug. Deliv. Rev.* **2001**, *46*, 3.

34. Di, L.; Kerns, E. H.; Fan, K.; McConnell, O. J.; Carter, G. T. *Eur. J. Med. Chem*. **2003**, *38*, 223.

35. Fernández-Bachiller, M. I.; Pérez, C.; Monjas, L.; Rademann, J.; Rodríguez-Franco, M. I. *J. Med. Chem*. **2012**, *55*, 1303.

36. Luo, Z.; Sheng, J.; Sun, Y.; Lu, C.; Yan, J.; Liu, A.; Luo, H. B.; Huang, L.; Li, X. *J. Med. Chem*. **2013**, *56*, 9089.

37. Lu, C.; Guo, Y.; Yan, J.; Luo, Z.; Luo, H. B.; Yan, M.; Huang, L.; Li, X. *J. Med. Chem*. **2013**, *56*, 5843.

Legends

Fig 1. Structures of the benzyloxy substituted MAO-B inhibitors 1-31.

Fig 2. Synthesis of the benzyloxy substituted derivatives 1-31. Reagents and conditions: (a) H_2, Pd/C, MeOH/EtOAc, 24 h; (b) $H_2SO_4/NaNO_2$; 50% H_2SO_4, 125 °C; (c) CF_3SO_3H, 75-80 °C, 1.5 h; (d) $ZnCl_2$, 50 °C, 2 h; (e) dioxane, conc. H_2SO_4, 90 °C, 4 h; (f) K_2CO_3, acetonitrile, reflux, 8 h.

Fig 3. Cytotoxicity and neuroprotective effects of the tested compounds 1-31. Survival data are expressed as the percentage of 6-OHDA- and rotenone-treated cells. Symbols represent significant changes from 6-OHDA- and rotenone-treated PC12 cells (*P < 0.05; **P < 0.01), respectively. All data are the means ± SEM of at least five values measured in two independent plates.

Fig 4. Neuroprotective effects of compound 13 against 6-OHDA- and rotenone-induced toxicity in PC12 cells. Rasagiline was used as the reference compound. Results are expressed as percent viability compared to cells not treated with neurotoxins. All data are the means ± SEM of at least five values measured in two independent plates (*P < 0.05; **P < 0.01).

Fig 5. Effects of compound 13 on 6-OHDA-induced apoptosis in PC12 cells. Symbols represent significant changes (**P < 0.01; ***P < 0.001).

Fig 6. Effects of compound 13 on rotenone-induced apoptosis in PC12 cells. Symbols represent significant changes (**P < 0.01; ***P < 0.001).

Fig 7. Effect of 13 against ROS generation was measured by DCFH-DA staining and analyzed by flow cytometry. Analysis of ROS production is presented as the mean fluorescence intensity (MFI). (*P < 0.05; **P < 0.01; ***P < 0.001).

Fig 7. Effects on body weight of mice fed 13 in the acute toxicity test.

Table 1. Inhibition of human MAO-A and MAO-B activities and neuroprotective effects of compounds 1-31.

Table 2. Physical properties and ADMET prediction of the selected compounds.

Table 3. Permeability results ($Pe \times 10^{-6}$ cm s^{-1}) from the PAMPA-BBB assay for selected compounds with their predicted penetration into the CNS.

Graphical Abstract:

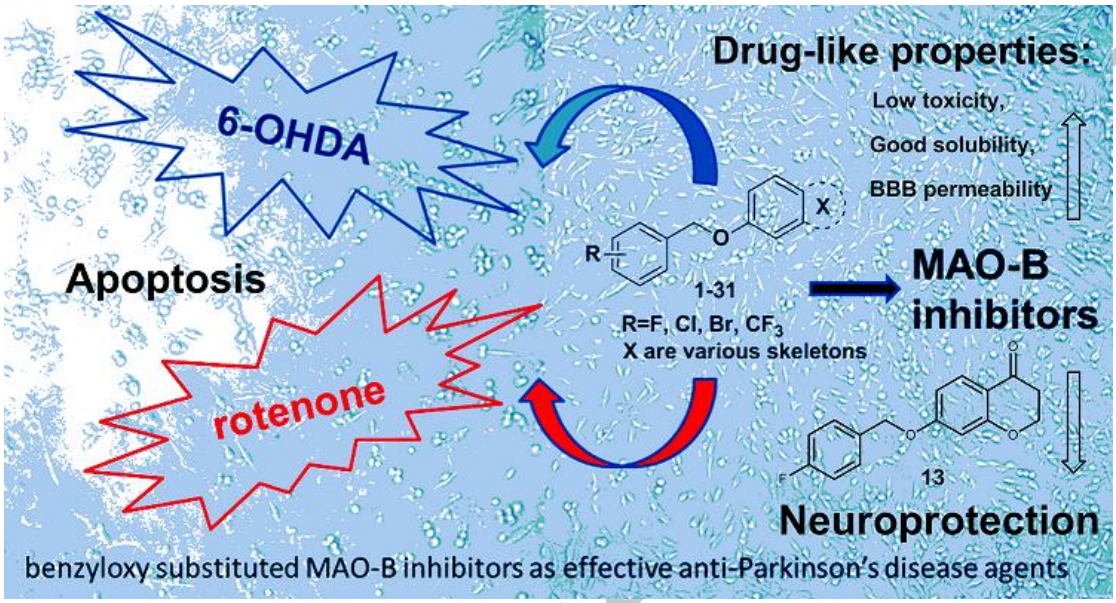

Highlights

- A series of representative benzyloxy substituted MAO-B inhibitors were synthesized and evaluated.
- Compounds **5-8**, **12-17**, **25**, **28** and **31** exhibited neuroprotective effects against 6-OHDA- and rotenone-treated PC12 cells.
- Compound **13** showed neuroprotective effects against neurotoxins-induced ROS accumulation and apoptosis.
- Compound **13** might be promising candidates for the therapy of Parkinson's disease.